Relativistic Ray Tracing: Visualizing Curved Space-Time Towards Locating Neutron Stars

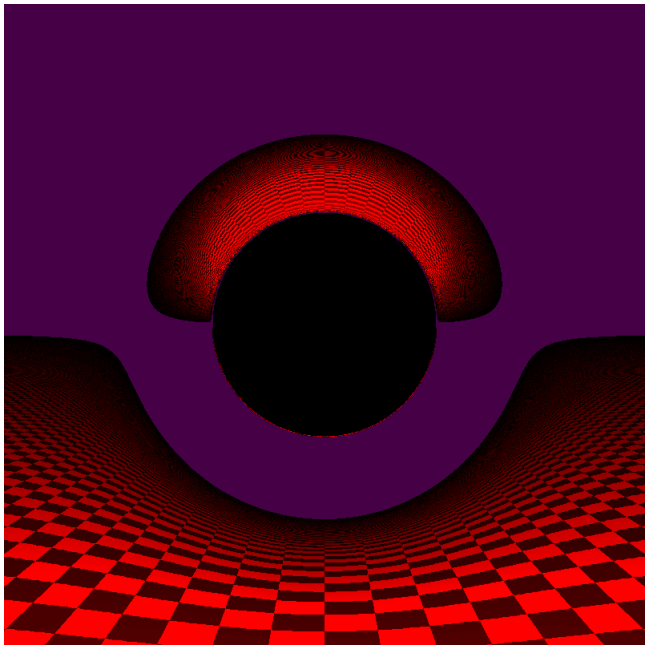

Austin Erickson

An undergraduate thesis advised by Kathryn Z. Hadley,
submitted to the Department of Physics, Oregon State University
in partial fulfillment of the requirements for the degree BS in Physics.

Submitted on May 12, 2023

Abstract

The study of neutron stars offers an opportunity to examine matter under extreme gravitation. Various methods have been developed to locate neutron stars such as the detection of electromagnetic pulses, gravitational waves, and radioactivity from supernova remnants. However, locating neutron stars still proves challenging.

We propose a method of locating neutron stars that leverages ray tracing to model light transport and generate an image set of star fields containing neutron stars. We seek to utilize this image set to train a machine learning algorithm to recognize and locate neutron stars in real images.

Neutron stars are approximated as compact masses which obey the Schwarzschild metric. By generating a field of stars that are sufficiently far from each other, the space-time between them is well approximated as flat. The equations of motion of massless particles are derived from the metric, and photon trajectories are solved numerically.

Contents

Figures

Introduction

2.1 Current Detection Methods

Current methods for identifying neutron stars include the detection of electromagnetic waves emitted by neutron stars[1], gravitational wave signals[2], and radioactive decay from supernova remnants[3, 4]

The detection of electromagnetic waves is a common strategy for detecting neutron stars. Young active neutron stars that are rapidly rotating emit consistent radio signals. These neutron stars are referred to as pulsars[2]. Radio signals can be detected by satellite arrays and the data can be sorted and filtered to reveal patterns associated with pulsar emissions.

Gravitational waves are an effect predicted by Albert Einstein where ripples in space-time are generated by accelerated massive objects. In the case that two compact objects orbit each other, or if there is an asymmetry of a rotating compact object, gravitational waves are produced[1]. When a pair of compact objects such as two neutron stars orbit each other, or if a neutron star is not perfectly symmetric and is rapidly rotating, they produce ripples in space-time which may be detected on Earth.

Another approach is to locate neutron stars by examining the radioactivity of isotopes present in young supernova remnants[3, 4]. This method is effective for the location of young, isolated, radio-quiet neutron stars[4].

2.2 Using the Method of Ray Tracing

The methods mentioned depend on aspects that are not present with all neutron stars. However, extreme density is a universal property of neutron stars. Thus, relativistic ray tracing may serve as a complimentary method for finding neutron stars. By modeling gravitational effects on light trajectories, we seek to train a machine learning algorithm to identify distortions in real images and locate neutron stars.

Theory

We will first describe the underlying principles that will govern light's motion. This paper seeks not only to present a novel method for locating neutron stars, but to also equip the reader with the tools and knowledge to understand and replicate the methods used. For this reason, we have chosen to go over background information in detail.

3.1 Linear Ray Tracing

Ray tracing is a technique which seeks to model light transport. In linear ray tracing, light is assumed to be travelling through a medium in which its wavefront trajectory can be well approximated by a straight line in space. Therefore, light is often modeled as a vector.

A useful calculation in ray tracing is ray-surface intersection, where an intersection point is calculated given a ray and a surface. Since we will be dealing with stars it is useful to consider ray-sphere intersection. The intersection algorithm is demonstrated geometrically in figure 3.1 and is given in pseudo-code [5]:

```
def test_intersection(O, D, C, r):
    # calculates the ray-sphere intersection point P given
    # a ray position O, ray direction D,
    # sphere position C, and sphere radius r

    # make sure direction is normalized
    D = normalize(D)
```

```
L = O - C
tca = dot(L, D)

if (tca < 0):
    no intersection

r_squared = r**2
d_squared = dot(L, L) - tca**2

if (r_squared < d_squared):
    no intersection

thc = sqrt(r_squared - d_squared)
t0 = tca - thc

if (t0 < 0):
    no intersection

P = O + t0*D

return P
```

3.2 The Metric: Distances in Space-Time

We begin with the familiar distance equation, the Pythagorean theorem

$$s = \sqrt{x^2 + y^2 + z^2}, \tag{3.1}$$

where s is the distance. For convenience and aesthetic, this will be written as

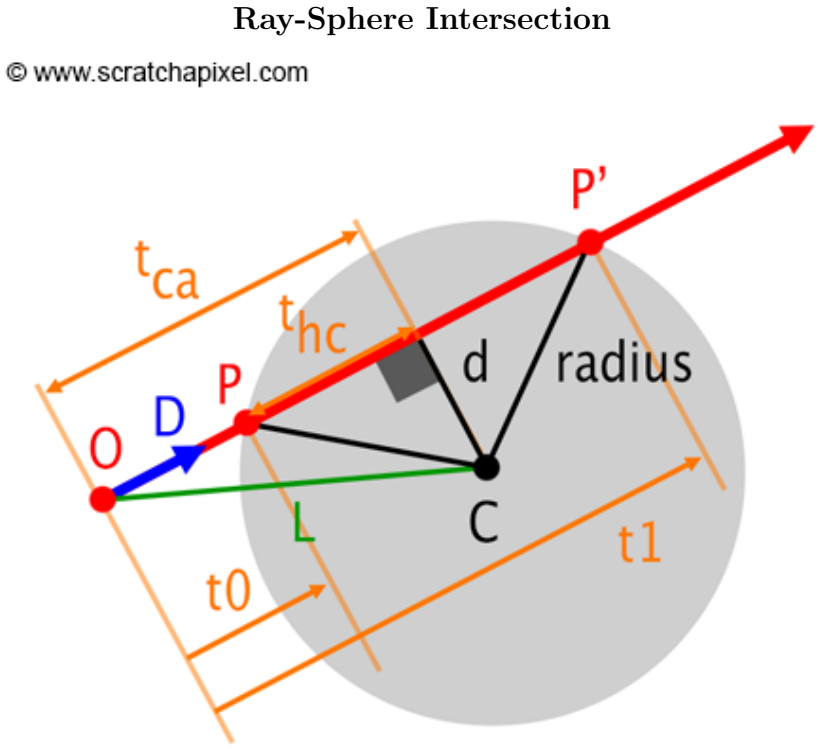

Figure 3.1: The intersection point created by a ray and a sphere may be derived geometrically. O is the ray origin. D is the ray direction. P and P' are the intersection points of the ray with the sphere. C is the sphere origin. L points from O to C. tca is the projection of L onto D. d squared is L squared minus tca squared. thc is the distance tca minus the distance from O to P. t0 is the distance from O to P. t1 is the distance from O to P'

$$s^2 = x^2 + y^2 + z^2. \tag{3.2}$$

In special relativity, distance is no longer given by the Pythagorean theorem. Since the speed of light is held constant, different observers will not agree in general on the place or time of an event, and will therefore not agree on distances (or times). Therefore, it is necessary to define a new distance. One in which all observers agree. This new distance is called the space-time distance such that

$$s^2 = -c^2t^2 + x^2 + y^2 + z^2. \tag{3.3}$$

It is a common convention to let $c \equiv 1$ for convenience. This is possible because letting c be 1 is just a change of coordinates, and we may convert back to standard dimensions at

any time. We will continue to use this convention for the rest of the paper. The distance now becomes

$$s^2 = -t^2 + x^2 + y^2 + z^2. \tag{3.4}$$

Such a distance relation is called the metric. This metric is commonly referred to as the flat space-time metric or the Minkowski metric, named after Hermann Minkowski.

There is a second way to calculate distance that is sometimes more useful. One can calculate distance by projecting a vector onto itself as follows:

$$|\vec{v}|^2 = \vec{v} \cdot \vec{v}. \tag{3.5}$$

This is advantageous because it is a coordinate free representation of distance.

When one takes the dot product of two vectors, one usually does the following:

$$\left\langle\ x_1, y_1, z_1\ \right\rangle \cdot \left\langle\ x_2, y_2, z_2\ \right\rangle = x_1x_2 + y_1y_2 + z_1z_2. \tag{3.6}$$

However, this is not the full story for two reasons. The first deals with the definition of the dot product. The true definition requires something called a "dual vector" or a "co-vector"[6]. For our purposes, the co-vector is simply the complex conjugate transpose. Thus, the dot product is more accurately represented as follows

$$\begin{bmatrix} x_1^* & y_1^* & z_1^* \end{bmatrix} \begin{bmatrix} x_2 \\ y_2 \\ z_2 \end{bmatrix} = x_1^*x_2 + y_1^*y_2 + z_1^*z_2, \tag{3.7}$$

where $*$ represents the complex conjugate.

At first glance, this definition of the co-vector may seem redundant. However, the real distinction between a vector and a co-vector is how they transform under coordinate change.

Consider a vector $\vec{r}$ in a Cartesian coordinate system where the basis is represented by $\hat{x}$ and $\hat{y}$ (figure 3.2)

If we are to transform the basis $\hat{x}$ and $\hat{y}$ by rotating by $\frac{\pi}{4}$ radians counter-clockwise, we see the vector now lies on the x-axis (figure 3.3).

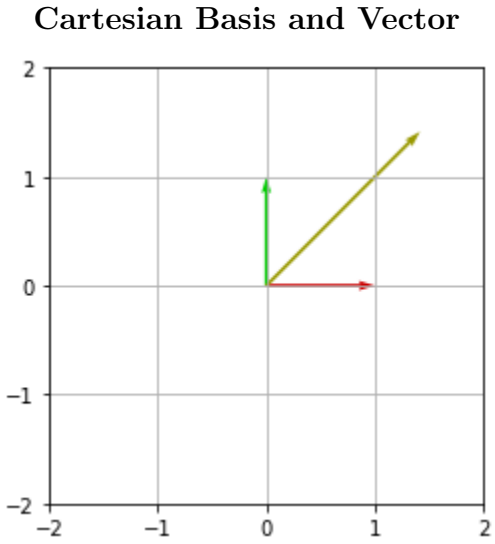

Figure 3.2: A basis is shown where $\hat{x}$ is represented in red, $\hat{y}$ is represented in green, and the vector $\vec{r}$ is represented in yellow.

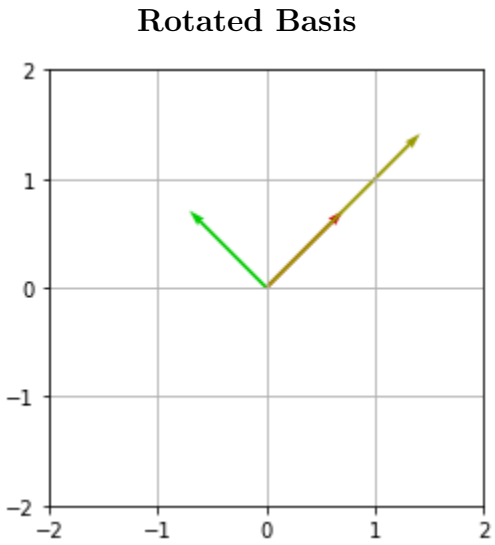

Figure 3.3: The basis is rotated with the vector fixed.

If we now instead transform the vector $\vec{r}$ by rotating it the same amount but clockwise, we see that the vector again lies on the x axis (figure 3.4).

These operations are inverses of each other, and thus the vector $\vec{r}$ is transforming opposite to the basis. Thus, we say that $\vec{r}$ is contra-variant. There are vector quantities that transform with the basis. These are referred to as co-variant. This distinction will become important later.

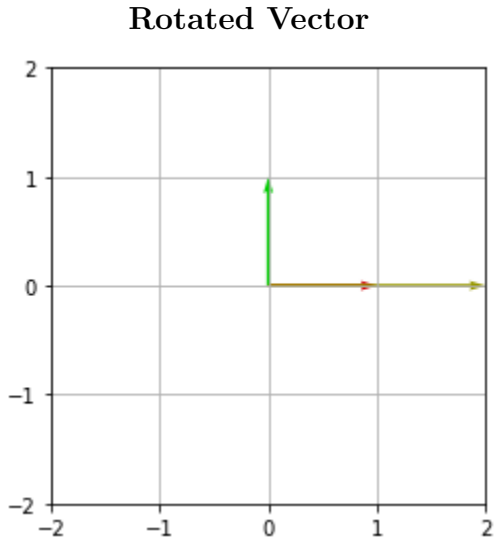

Figure 3.4: The basis is held fixed, and the vector is rotated in the opposite direction the basis was rotated.

The second reason is there is a hidden matrix every time a dot product is taken. This is because most dot products taken are such that

$$\begin{bmatrix} x_1^* & y_1^* & z_1^* \end{bmatrix} \begin{bmatrix} 1 & 0 & 0 \\ 0 & 1 & 0 \\ 0 & 0 & 1 \end{bmatrix} \begin{bmatrix} x_2 \\ y_2 \\ z_2 \end{bmatrix} = x_1^* x_2 + y_1^* y_2 + z_1^* z_2, \tag{3.8}$$

where the matrix in the center is the metric! Euclidean space has no curvature, and the metric is written in Cartesian coordinates, so the metric is simply the identity. In other words, distances (and angles) do not change depending on where we are in space.

In order to take a dot product in special relativity, simply insert the metric of special relativity in place of the metric for euclidean space as shown:

$$\begin{bmatrix} t_1^* & x_1^* & y_1^* & z_1^* \end{bmatrix} \begin{bmatrix} -1 & 0 & 0 & 0 \\ 0 & 1 & 0 & 0 \\ 0 & 0 & 1 & 0 \\ 0 & 0 & 0 & 1 \end{bmatrix} \begin{bmatrix} t_2 \\ x_2 \\ y_2 \\ z_2 \end{bmatrix} = -t_1^* t_2 + x_1^* x_2 + y_1^* y_2 + z_1^* z_2. \tag{3.9}$$

We now generalize the inner product distance method to space-time by projecting an

arbitrary position vector onto itself

$$s^2 = \begin{bmatrix} t^* & x^* & y^* & z^* \end{bmatrix} \begin{bmatrix} -1 & 0 & 0 & 0 \\ 0 & 1 & 0 & 0 \\ 0 & 0 & 1 & 0 \\ 0 & 0 & 0 & 1 \end{bmatrix} \begin{bmatrix} t \\ x \\ y \\ z \end{bmatrix} = -t^*t + x^*x + y^*y + z^*z, \tag{3.10}$$

where we have reproduced the space-time distance for special relativity

$$s^2 = -t^2 + x^2 + y^2 + z^2. \tag{3.11}$$

However, you may notice an immediate issue with this formula. Figure 3.5 represents a light cone where the diagonals are trajectories of light from the origin. The path of an observer at the origin is restricted to the light cone as it would require a speed greater than c to escape the region. This is equivalent to saying

$$t^2 >= x^2 + y^2 + z^2. \tag{3.12}$$

However, this means that equation 3.11 will return a complex value for distance. Thus, we define a new distance

$$\tau \equiv -s, \tag{3.13}$$

such that a new distance function

$$\tau^2 = t^2 - x^2 - y^2 - z^2, \tag{3.14}$$

will return a real number for distance [7]. This new distance corresponds to the time experienced by an observer following the path [what path? the path to the place the position vector points?]. This distance is thus referred to as the proper time (proper meaning "one's own"). This is equivalent to redefining the metric to be

$$\eta_{\alpha\beta} = \begin{bmatrix} 1 & 0 & 0 & 0 \\ 0 & -1 & 0 & 0 \\ 0 & 0 & -1 & 0 \\ 0 & 0 & 0 & -1 \end{bmatrix}. \tag{3.15}$$

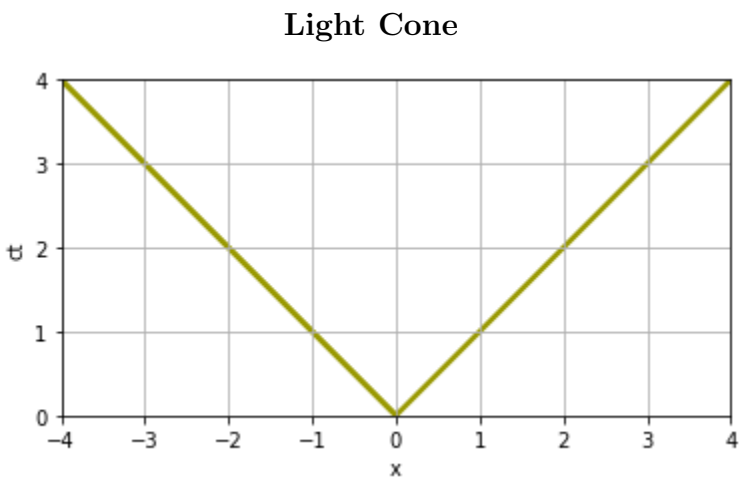

Figure 3.5: A light cone is shown in flat space-time.

It is a fact that all metrics in relativity will have either time-like components be negative and all space-like components be positive or vice-versa. This is called the metric signature. We will proceed with the [+ - - -] signature.

3.3 Gravity as Curvature

Now that we have the necessary theoretical foundation, we shift our attention to general relativity. In general relativity, space-time is less like a static flat sheet and more like a fabric that can stretched and deformed. According to general relativity, gravity is not a force. Rather, gravity is the curvature in space-time and the source of this curvature is the matter and energy present within it. This relationship is known as the Einstein field equation given by

$$R_{\mu\nu} - \frac{1}{2} g_{\mu\nu} R = 8\pi G T_{\mu\nu}, \tag{3.16}$$

which relates the curvature R of space-time and the matter and energy T within it [7].

To solve the Einstein field equation, one is tasked with finding the metric $g_{\mu\nu}$ given an arrangement of matter and energy. The field equation is sometimes referred to as the field equations because there are actually 16 equations as the indices of μ and ν each take on the values from 0, 1, 2, 3 corresponding to one time dimension and three spatial dimensions (this actually reduces to 10 due to redundancy). In addition, the field equation is a differential equation as matter and energy tells space-time how to curve, and the curvature of space-time tells matter and energy how to move. For this reason, we will take solutions as given. In particular, we will examine the Schwarzschild solution in the next section.

3.4 The Schwarzschild Metric

The Schwarzschild solution is an exact solution to Einstein's field equation. The Schwarzschild metric describes space-time outside compact, uncharged, spherically symmetric masses. In spherical coordinates t, r, θ, and ϕ (where θ is the azimuthal angle), the metric may be represented as

$$g_{\mu\nu} = \begin{bmatrix} (1-\frac{r_s}{r}) & 0 & 0 & 0 \\ 0 & -\frac{1}{(1-\frac{r_s}{r})} & 0 & 0 \\ 0 & 0 & -r^2 & 0 \\ 0 & 0 & 0 & -r^2 sin^2(\theta) \end{bmatrix}, \tag{3.17}$$

where r_s is the Schwarzschild radius (the radius of a black hole of identical mass), r is the coordinate radius[7]. Notice that the metric's entries are functions. This means that distances depend on position. The flat space-time metric does not change with position so we did not have to concern ourselves with calculus. Now, we will need to calculate local, infinitesimal distances and sum them along the path of interest. The local distance between neighboring points in Schwarschild space-time is given by the metric as follows

$$d\tau^2 = \left(1-\frac{r_s}{r}\right)dt^2 - \frac{1}{(1-\frac{r_s}{r})}dr^2 - r^2 d\theta^2 - r^2 sin^2(\theta) d\phi^2. \tag{3.18}$$

If one can find a parametrization for the curve, the distance along the curve may be found

through integration. The following section will cover a special class of curves in space-time that seeks to minimize local distances.

3.5 Geodesics

The trajectory of light in flat geometry can be described as a straight line. In curved space-time, light's trajectory also follows a "straight line". That is, it follows the straightest line possible on a curved space-time. This "straightest line" is a concept known as a geodesic.

Consider an ant on a sphere. Imagine the ant wishes to walk forward in a straight line. It starts taking steps in the direction it faces and without changing direction eventually reaches the spot where it started. This "straightest path" the ant just walked is called a great circle and is the geodesic for a sphere.

In general relativity, the geodesic is the path an objects takes in space-time when free of any external forces. Thus, the equations of motion for a free-falling body may be derived by utilizing the calculus of variations. The derivation will not be discussed in this paper, but the result is given by

$$\frac{d^2x^\lambda}{d\tau^2} = -\Gamma^\lambda_{\mu\nu}\frac{dx^\mu}{d\tau}\frac{dx^\nu}{d\tau}, \tag{3.19}$$

where the Γ coefficients are referred to as "Christoffel symbols" or "affine connection" coefficients. These coefficients can be found directly from the metric and its derivatives, but this will not be necessary for our applications.

This equation is known as the geodesic equation. Notice the superscripts. These are indices, not powers. Thus, $\Gamma^\lambda_{\mu\nu}$ is represented by a 4x4x4 matrix. The superscript index is used to distinguish between contra-variant and covariant (discussed in the metric section). Lower indices represent co-variant and upper indices represent contra-variant.

x in this equation represents all coordinates. For example, if a Cartesian basis was chosen,

$$
\begin{aligned}
x^0 &= t, \\
x^1 &= x, \\
x^2 &= y, \\
x^3 &= z.
\end{aligned}
\tag{3.20}
$$

Another important note is that this equation actually consists of 4 equations, 3 for space and 1 for time denoted by λ, which takes the values 0, 1, 2, 3. These equations are a sum over all possible combination of the indices μ and ν. So each equation will have 16 terms. This is referred to as Einstein summation notation, where repeated indices are summed over.

Next, take notice of the form of the equation. On the left there is a second order space derivative with respect to proper time. On the right, the connection coefficients and two first order space derivatives with respect to proper time. This equation tells us that the "acceleration" is given by the product of the connection coefficients (derived from the metric) and the "velocity". In other words, the acceleration of a free-falling object moving through space-time is dependant solely on its velocity and the shape of space-time, no forces needed!

3.6 Hamiltonian Approach

The geodesic equation derived from the Euler-Lagrange equation has two problems. The first is that we have a parametrization of proper time. This is an immediate problem as light follows null geodesics in space-time. In other words, the proper time change of light is $d\tau = 0$, resulting in a mapping between the parameter and curve that is not one-to-one. We will return to this issue later by introducing something called an affine parameter.

The second problem is that the form of the differential equation is second order. To solve numerically it will be beneficial to put the equation into a form in which it is first order. This is possible through the Hamiltonian approach.

The following derivation is an expanded explanation for the research paper "Non-linear Monte Carlo Ray Tracing for Visualizing Warped Spacetime" by Avirup Mandal et al.[8]. So that the paper may flow better, intermediate steps are omitted from the derivation. See the appendix for the full derivation.

The Hamiltonian may be written as

$$\mathscr{H} = \frac{1}{2} g^{\mu\nu} p_\mu p_\nu, \tag{3.21}$$

which allows us to rewrite the second order equation of motion into two equivalent first order equations of motion. Since proper time cannot be used as a parameter for light, we will assign an arbitrary affine parameter ζ

$$\frac{dx^\alpha}{d\zeta} = \frac{\partial \mathscr{H}}{\partial p_\nu} = g^{\alpha\nu} p_\nu, \tag{3.22}$$

$$\frac{dp_\alpha}{d\zeta} = -\frac{\partial \mathscr{H}}{\partial x^\alpha} = -\frac{1}{2} \frac{\partial g^{\mu\nu}}{\partial x^\alpha} p_\mu p_\nu. \tag{3.23}$$

We may now derive the equations of motion given a metric. We will of course use the Schwarschild metric. However, for our purposes it is advantageous to use isotropic Schwarzschild coordinates as this will enable us to ray trace easily with a camera that uses Cartesian coordinates for screen positions.

The covariant metric may be written as

$$g_{\mu\nu} = \begin{bmatrix} (\frac{1-\frac{r_s}{4r}}{1+\frac{r_s}{4r}})^2 & 0 & 0 & 0 \\ 0 & -(1+\frac{r_s}{4r})^4 & 0 & 0 \\ 0 & 0 & -(1+\frac{r_s}{4r})^4 & 0 \\ 0 & 0 & 0 & -(1+\frac{r_s}{4r})^4 \end{bmatrix}. \tag{3.24}$$

The metric is defined such that

$$g^{\mu\alpha} g_{\alpha\nu} = \delta^\mu_\nu. \tag{3.25}$$

In other words, the contra-variant and co-variant metrics are inverses of each other. Since the metric is diagonal, the contra-variant metric entries are simply the reciprocal of the co-variant metric entries

$$g^{\mu\nu} = \begin{bmatrix} (\frac{1-\frac{r_s}{4r}}{1+\frac{r_s}{4r}})^{-2} & 0 & 0 & 0 \\ 0 & -(1+\frac{r_s}{4r})^{-4} & 0 & 0 \\ 0 & 0 & -(1+\frac{r_s}{4r})^{-4} & 0 \\ 0 & 0 & 0 & -(1+\frac{r_s}{4r})^{-4} \end{bmatrix}. \tag{3.26}$$

We start with time

$$\frac{dp_0}{d\zeta} = -\frac{1}{2}\frac{\partial g^{\mu\nu}}{\partial x^0} p_\mu p_\nu, \tag{3.27}$$

but the metric does not change with time. Thus,

$$\frac{dp_0}{d\zeta} = 0, \tag{3.28}$$

which implies p_0 is constant, and we may define it to be

$$p_0 \equiv -1. \tag{3.29}$$

Now,

$$\frac{dx^0}{d\zeta} = g^{0\nu} p_\nu = \left(\frac{1-\frac{r_s}{4r}}{1+\frac{r_s}{4r}}\right)^{-2} p_0, \tag{3.30}$$

since the metric is diagonal. Using our definition from before,

$$\frac{dx^0}{d\zeta} = -\left(\frac{1-\frac{r_s}{4r}}{1+\frac{r_s}{4r}}\right)^{-2}. \tag{3.31}$$

For $\alpha = 1, 2, 3$,

$$\frac{dx^\alpha}{d\zeta} = \left(1+\frac{r_s}{4r}\right)^{-4} p_\alpha, \tag{3.32}$$

$$\frac{dp_\alpha}{d\zeta} = \frac{1}{2r^3}\left[\frac{p^2}{(1+\frac{r_s}{4r})^5} + \frac{(1+\frac{r_s}{4r})}{(1-\frac{r_s}{4r})^3}\right] r_s x^\alpha. \tag{3.33}$$

We have discovered that

$$\frac{dx^0}{d\zeta} = -\left(\frac{1-\frac{r_s}{4r}}{1+\frac{r_s}{4r}}\right)^{-2}, \tag{3.34}$$

and by definition

$$\frac{dx^0}{d\zeta} = \frac{dt}{d\zeta}. \tag{3.35}$$

Thus,

$$\frac{d\zeta}{dt} = -\left(\frac{1-\frac{r_s}{4r}}{1+\frac{r_s}{4r}}\right)^{2}. \tag{3.36}$$

We may now apply the chain rule to re-parameterize the equations of motion in terms of t.

for $\alpha = 1, 2, 3$,

$$\frac{dx^\alpha}{dt} = \frac{(1-\frac{r_s}{4r})^2}{(1+\frac{r_s}{4r})^6} p_\alpha, \tag{3.37}$$

$$\frac{dp_\alpha}{dt} = -\frac{1}{2r^3}\left[\frac{(1-\frac{r_s}{4r})^2}{(1+\frac{r_s}{4r})^7}p^2 + \frac{1}{(1+\frac{r_s}{4r})(1-\frac{r_s}{4r})}\right] r_s x^\alpha. \tag{3.38}$$

These equations may now be solved numerically to find the path a photon takes near a compact mass.

Now, equipped with the tools we require, we begin our task of modeling light in curved geometry.

Methods

4.1 Assumptions

We begin with assumptions. General relativity is a complex subject as has been made clear by the (brief) theoretical overview. The following assumptions will reduce many of the challenges ahead. We assume a spherically symmetric compact mass that does not rotate, is quasi-static (mostly stationary), and that stars are placed far enough away from neighboring stars that the space-time between them can be considered Minkowskian (flat). It is true that real neutron stars can rotate rapidly. However, this assumption enables us to use the Schwarzschild metric which will greatly simplify ray tracing.

The advantage of assuming distances are large is that it allows one to create ray traced images involving more than one star, which is important for displaying gravitational effects on light. This can be done by effectively translating the center of a mass by shifting the coordinate position in the equations of motion.

It is important to emphasize that one cannot just add two metrics together to produce a new metric. Rather, in the limit as the distance between masses becomes very large, the metric approaches the Minkowski metric. Thus, for two stars with large distances between each other, the metric can be considered flat. This approximation will allow for the calculation of light trajectories in a space-time filled with distant stars.

4.2 Relativistic Ray Tracing

The advantage to using the ray tracing method is that with minor modification it can be made to evolve a photon in a non-linear way. The algorithm in Figure 4.1 details the steps required to evolve a photon in curved space-time. For every pixel we will assign an initial ray based upon the position and momentum of the photon. Next, a test is performed to check that the photon did not begin inside a sphere. If not, we check whether the photon is within a sphere of influence (SOI). This is a spherical region centered on a massive sphere such that the gravitation is significant and space-time cannot be treated as flat. If the photon is outside an SOI, we check if it will intersect one at some later time. If not, we check if it will intersect a sphere. If yes, the intersection is performed and the surface color is returned. If not, the background color is returned.

If the photon starts within a mass (Figure 4.2), an error color will be returned. If the photon is not initially in a mass and it is in a sphere of influence (Figure 4.3), the photon is integrated according to the equations of motion. During the integration, a check is performed on intersection with the surface of the mass (Figure 4.4). If intersection occurs during integration, the surface color is returned. If the photon escapes the sphere of influence, we check for sphere of influence intersection and mass intersection and repeat the steps from before (Figures 4.5, 4.6).

Figure 4.7 depicts two scenarios. One in which a ray comes under influence of a mass, and intersects with its surface. The other in which the ray comes under influence of a mass, leaves the mass's influence without intersecting its surface, comes under influence of a second mass, leaves its influence, and intersects with a mass in which its sphere of influence is within its surface. While the ray is outside a sphere of influence, a linear ray trace is performed to either the next sphere of influence, or to a mass's surface (if the sphere of influence is smaller than its surface). If neither of these conditions exist, then there is no intersection and the background color is returned.

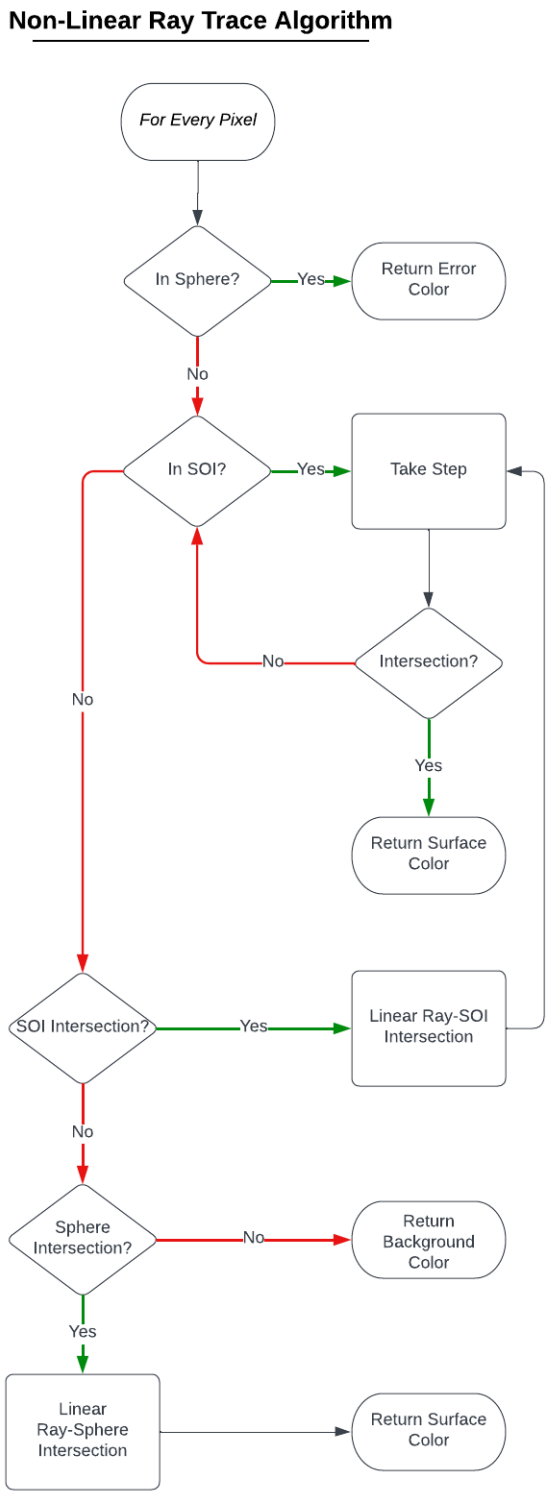

Figure 4.1: A photon's path may be evolved in curved space-time by combining standard linear ray tracing methods and integrating the equations of motion.

In Mass

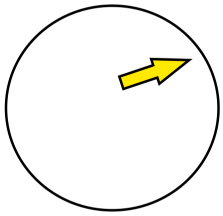

Figure 4.2: Photon within a mass.

In SOI

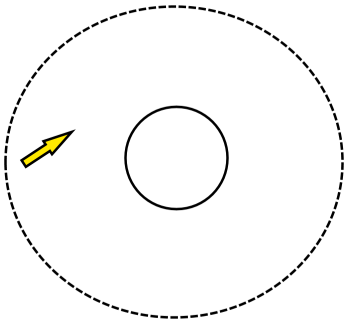

Figure 4.3: Photon within SOI.

Non-Linear Mass Intersection

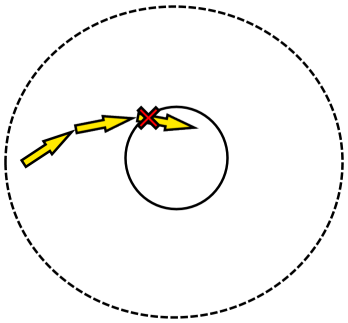

Figure 4.4: A linear ray intersection test during integration of the ray in an SOI resulting in a ray SOI intersection

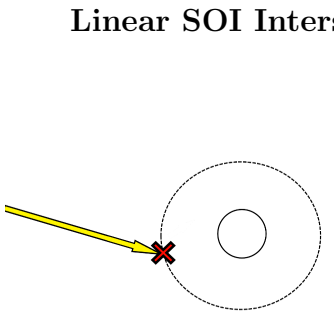

Figure 4.5: A linear ray intersection test resulting in a ray SOI intersection.

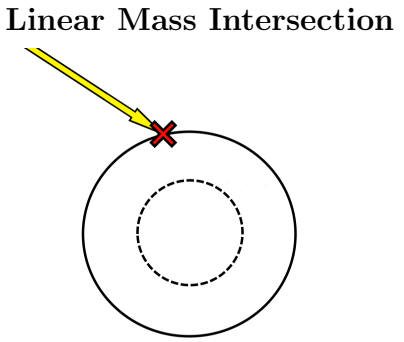

Figure 4.6: A linear ray intersection test resulting in a ray mass intersection.

Algorithm Visualization

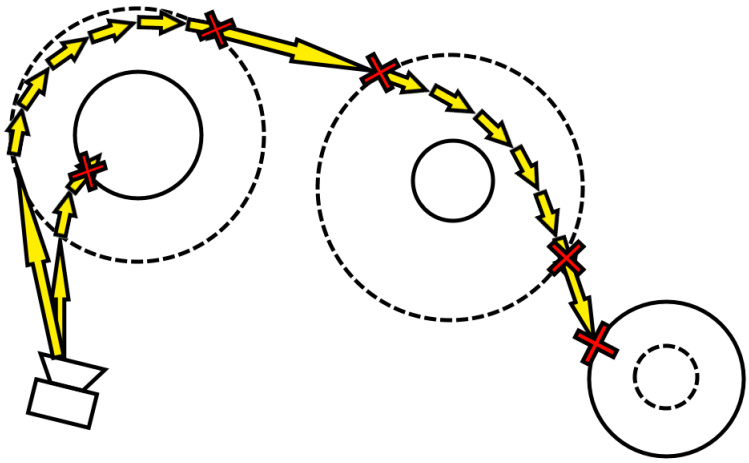

Figure 4.7: Two paths are shown depicting how a photon evolves using the relativistic ray tracing algorithm. One evolves with linear ray-SOI intersection, is integrated in the SOI, and intersects with the mass's surface. The second ray evolves in a similar manner, but leaves the SOI. A linear ray-SOI intersection is performed, the ray is integrated and leaves the sphere of influence. A ray-mass intersection occurs with a mass that has an SOI radius smaller than its mass radius.

Results and Discussion

5.1 Generated Images

In the relativistic ray tracing section, you may have noticed that the ray directions point from the camera into the world. This is counter-intuitive, but necessary. In real life, light is emitted from light sources, and light travels to our eye. If we were to model light in this way, a very large number of rays would need to be generated to intersect with a small number of pixels since the intersection with pixel centers is rather unlikely. Because of this, the ray tracing method works backwards, generating the light rays at the pixel centers and evolving them into the world. Whatever the ray intersects is what is seen. This creates a one-to-one mapping between pixels and colors. For the following discussion, we will adopt the perspective that what we see is what the photon strikes.

When we see the world, we make an assumption that the light we are seeing is travelling in a straight line. When this assumption is incorrect, we anticipate the location of objects to be in places they are not. More specifically, we expect them to be at some distance along the tangent line of the light at the point it makes contact with our eye. An example of this is a straw in a water glass. The straw will appear bent in the water, despite being straight. This effect becomes very apparent when examining compact masses and their distortions on light's trajectory.

For example, the north and south poles of a compact massive sphere will be simultaneously visible to an observer. This is because the light bends in towards the object when it would classically continue in a straight path. This results in one being able to see more of

the surface at once than would normally be possible. In addition, it makes the apparent size of the object appear larger. This is because the light that would normally escape intersects with the surface of the object, and thus the object will take up more of one's field of view.

Successfully modeling this behavior was the first test of validity. We placed a compact mass with a radius of it's Schwarzschild radius (a black hole) in a scene and set a camera at a distance pointed towards it. The generated image is given in figure 5.1, and returns the expected results that the north and south pole of the object is visible simultaneously, and that the apparent size is enlarged.

The Apparent Surface of a Black Hole

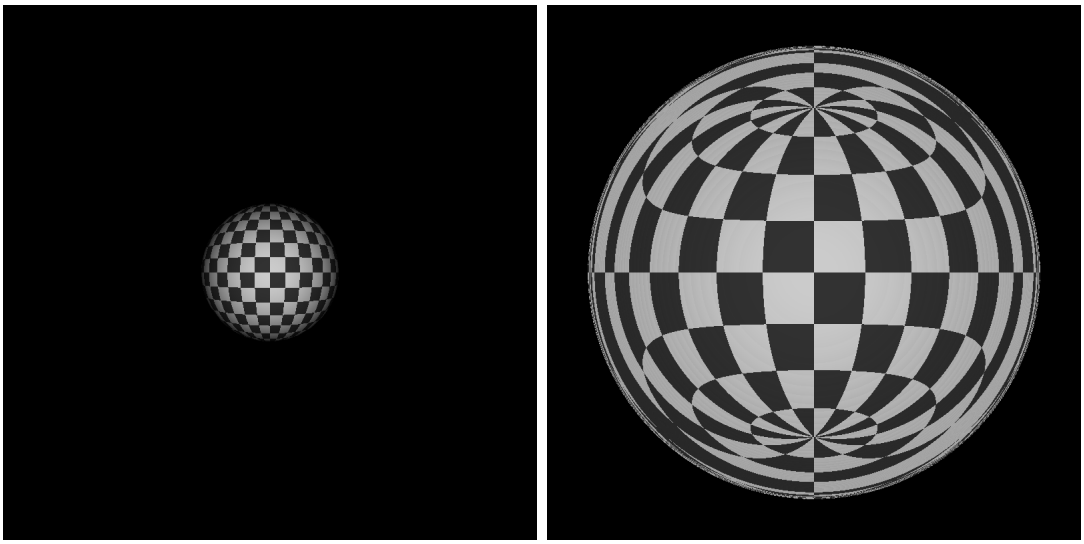

Figure 5.1: The checkered surface a black hole is shown. The north and south pole are visible simultaneously, and the apparent size appears enlarged.

The second test we performed was placing a star behind a compact mass, such that the star would be entirely hidden behind the compact mass classically. Since light bends near compact masses, we expect the star to be visible from behind the relativistic object. The gravitational lensing results in a phenomena known as an "Einstein ring", where the light of the star is warped into a ring shape surrounding the compact mass such that it is visible to an observer despite being behind the compact mass. When a black hole is placed in front of a star in a scene in the model, the resulting image, seen in figure 5.2, agrees with the expected result.

By analyzing figure 5.2, one can reason why the light takes the form of a ring by con-

sidering the path of light from the camera to the star. The purple background is where the light does not intersect, the yellow is where the light intersects the star, and the black is where the light intersects the black hole event horizon.

As the light leaves the camera, it is bent towards the black hole. If the light is bent enough, it falls in. If it is bent to a lesser extend it will escape into the scene. If it is bent in just the right range, it will intersect with the star. If it is bent any less, it will not be bent enough to intersect with the star and will escape into the scene. This is why there is a spacing between the black hole and the ring.

Star Behind Black Hole

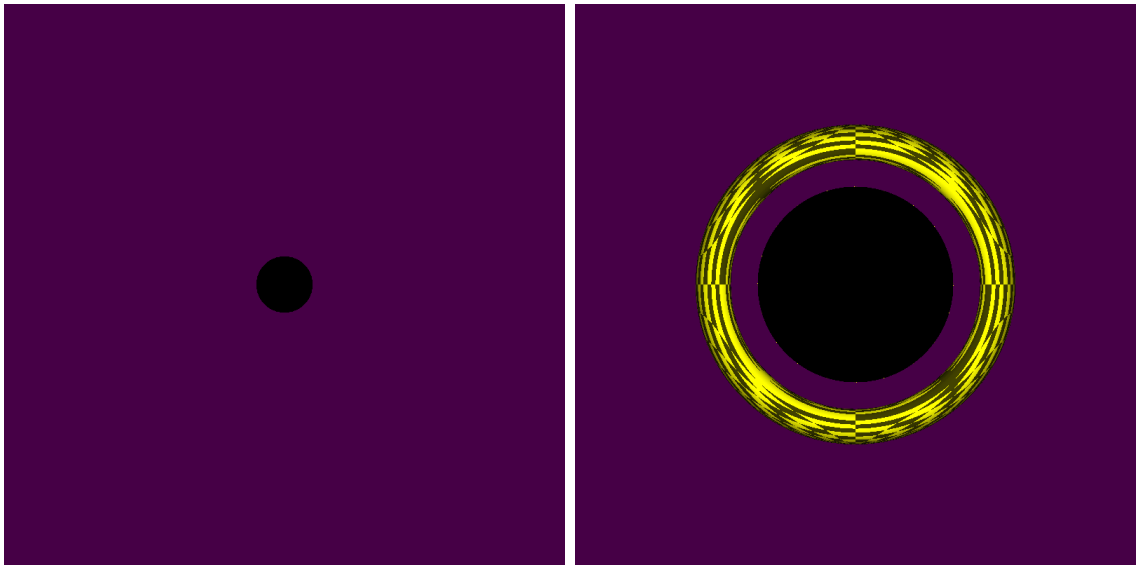

Figure 5.2: A black hole is placed so that it blocks a star behind it in the left image. The right image shows the same scene, but accounting for the bending of light.

Finally, we use the model to produce an image of a neutron star in front of a field of stars. This was done by "randomly" placing stars that were sufficiently non-relativistic behind a neutron star (compact mass of radius 1.5 of its Schwarzschild radius), where "random" placement accounts for the restriction that stars are sufficiently far so that the space-time between them can be approximated as flat.

The result was as expected. As seen in figure 5.3, the stars in the background are elongated and wrap around the compact mass in a shape characteristic of the previously discussed Einstein ring, reassembling the form of gravitational lensing effects in satellite images.

Gravitational Lensing in a Stellar Field

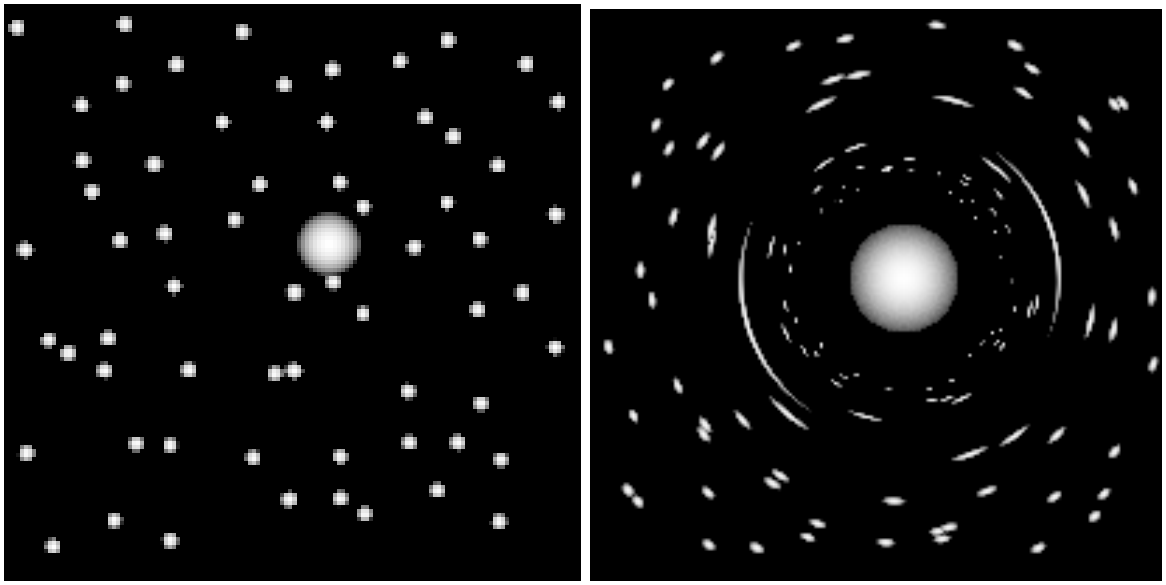

Figure 5.3: A neutron star is placed in front of a stellar field. The image on the left assumes light follows a strait path. The image on the right accounts for the light bending.

5.2 Future Prospects

5.2.1 Machine Learning

With a working model, we plan to generate two data sets. One of images of scenes including non-relativistic objects, and another of scenes including non-relativistic and relativistic objects. After combining the sets and splitting into training and testing sets, we plan to train a machine learning algorithm to recognize relativistic objects in scenes. Once it is clear that the machine learning algorithm works, we seek to apply it to real images to detect and locate neutron stars.

5.2.2 Refining the Model

There were many assumptions made in the development of the model. Thus, there are many refinements that could be made to the model to better represent reality. Assumptions regarding masses include non-rotating, which is an unrealistic assumption for neutron stars, uncharged , and large distances from each other, which is unrealistic because binary star

systems are not uncommon.

Of these assumptions the most concerning is the non-rotating assumption. This assumption may be fixed by switching the equations of motion to a set derived from the Kerr metric (as apposed to the Schwarzschild metric). However, this assumption was made to greatly simplify the model. In order to incorporate rotating masses, one would need to derive the new equations of motion and implement them, which would pose a challenge since the Kerr equations of motion would be in spherical coordinates. It would also be necessary to consider the validity of a sphere of influence when gravitational effects would not be spherically symmetric. The geometry of the spinning object would also have to be re-examined for proper ray intersection as the object may no longer be a sphere. The greatest challenge this presents is the time dependent metric. In the current model, everything is treated as static as the metric does not depend on time. However, one would likely need to ray trace in all four dimensions to accurately portray a scene with rotating masses.

The single star system assumption likely has less significant effects on the model's accuracy, but would be a far more challenging problem to resolve. Since metrics cannot be linearly super-positioned, one would need to find a solution (or a good approximation) for binary systems, or calculate the metric and equations of motion numerically for each frame within the influence of the binary system, which would be very computationally expensive.

5.2.3 Programming Language

Another consideration is the programming language. One could speed up the program by creating a version of the code in C or another similar low-level language.

However, the code used to generate images in this paper was not designed with high speed in mind. The code was designed for readability and easy debugging and modification, which is why the code was written in Python.

A compromise could be to vectorize the code. Since numpy is written mostly in C, performing matrix operations using numpy, especially when the operations are performed on large data sets, often yields higher performance than performing operations in Python alone.

A problem with this is that the operations performed on the rays (after setup) depend

on position, and is thus non-linear. Therefore, a single matrix operation being applied to all rays simultaneously would be more difficult to implement.

5.2.4 GPU Acceleration

In addition, it is possible to accelerate the process with a graphics card. Despite the ray integration requiring values that depend on the previous step, each ray itself is independent of the others. Thus, the problem can be parrallelized. The primary reason this approach was not used is that it is much harder to implement object orientation on a GPU, and the object orientation structure is extremely helpful in organizing and generalizing the ray tracing process for many objects. Another consideration against GPU acceleration was that a CPU cluster could perform the same task in a similar time-frame without the complications of programming a GPU.

Conclusion

We have produced a program that generates images of compact masses accounting for curvature of space-time. This is done by calculating the paths that photons take in space-time, calculating the intersection point of the photon with masses in the scene, and calculating the color of the pixel associated with the photon. The program was generalized to handle any number of masses sufficiently far from each other.

The images generated showcase and visualize the effects of curved space-time on light near compact masses. The model passes tests such as the simultaneous visibility of the north and south pole, the visibility of a star behind a compact mass, and successfully produces Einstein rings around compact masses in a stellar field.

We seek to utilize this model to generate a data set to train a machine learning algorithm to detect neutron stars in real images. By generating two sets of images of stellar fields, one of which includes no compact masses and one which includes some compact masses, we hope to train the machine learning algorithm to distinguish between images which have relativistic effects and ones that do not. This would allow for fast sifting of real images to locate neutron stars.

In addition, we seek to refine the model. Many assumptions were made in the making of the model such as non-rotating, uncharged, distant masses. Since neutron stars rotate rapidly, and binary star systems are common place, these assumptions are simplistic but inaccurate. We expect a more refined model to yield better training data for a machine learning algorithm.

References

[1] Marlin B. Schäfer, Frank Ohme, and Alexander H. Nitz. Detection of gravitational-wave signals from binary neutron star mergers using machine learning. *American Physical Society*, 2020.

[2] NASA. Neutron stars. https://imagine.gsfc.nasa.gov/science/objects/neutron$_stars1.html$(2021).

[3] Markus M. Hohle, Ralph Neuhäuser, and Nina Tetzlaff. Using radioactivities to improve the search for nearby radio-quiet neutron stars.

[4] Andrea De Luca. Central compact objects in supernova remnants. *arXiv*, 2007.

[5] Scratchapixel. Ray-sphere intersection. https://www.scratchapixel.com/lessons/3d-basic-rendering/minimal-ray-tracer-rendering-simple-shapes/ray-sphere-intersection.html.

[6] Sergei Treil. *Linear Algebra Done Wrong.* 2004.

[7] James Hartle. *Gravity An Introduction to Einstein's General Relativity.* Pearson Education, 2003.

[8] Avirup Mandal, Kumar Ayush, and Parag Chaudhuri. Non-linear monte carlo ray tracing for visualizing warped spacetime. *CITEPRESS*, 2021.

Appendix

The code for this project may be found by using the following link:

`https://github.com/AustinErickson/relativistic_ray_tracer`

Schwarzschild Metric (Spherical Coordinates)

$$g_{\mu\nu} = \begin{bmatrix} (1 - \frac{r_s}{r}) & 0 & 0 & 0 \\ 0 & -\frac{1}{(1-\frac{r_s}{r})} & 0 & 0 \\ 0 & 0 & -r^2 & 0 \\ 0 & 0 & 0 & -r^2 sin^2(\theta) \end{bmatrix} \tag{7.1}$$

$$g^{\mu\nu} = \begin{bmatrix} \frac{1}{(1-\frac{r_s}{r})} & 0 & 0 & 0 \\ 0 & -(1 - \frac{r_s}{r}) & 0 & 0 \\ 0 & 0 & -\frac{1}{r^2} & 0 \\ 0 & 0 & 0 & -\frac{1}{r^2 sin^2(\theta)} \end{bmatrix} \tag{7.2}$$

Schwarzschild Metric (Isotropic Coordinates)

$$g_{\mu\nu} = \begin{bmatrix} (\frac{1-\frac{r_s}{4r}}{1+\frac{r_s}{4r}})^2 & 0 & 0 & 0 \\ 0 & -(1 + \frac{r_s}{4r})^4 & 0 & 0 \\ 0 & 0 & -(1 + \frac{r_s}{4r})^4 & 0 \\ 0 & 0 & 0 & -(1 + \frac{r_s}{4r})^4 \end{bmatrix} \tag{7.3}$$

$$g^{\mu\nu} = \begin{bmatrix} (\frac{1-\frac{r_s}{4r}}{1+\frac{r_s}{4r}})^{-2} & 0 & 0 & 0 \\ 0 & -(1+\frac{r_s}{4r})^{-4} & 0 & 0 \\ 0 & 0 & -(1+\frac{r_s}{4r})^{-4} & 0 \\ 0 & 0 & 0 & -(1+\frac{r_s}{4r})^{-4} \end{bmatrix} \tag{7.4}$$

$$r^2 = x^2 + y^2 + z^2 \tag{7.5}$$

The derivative of the time component of the metric with respect to the spatial coordinates can be written as

$$\begin{aligned} \frac{\partial g^{00}}{\partial x^\alpha} &= \frac{\partial}{\partial x^\alpha}[(1-\frac{r_s}{4r})^{-2}(1+\frac{r_s}{4r})^2] \\ &= \frac{\partial}{\partial x^\alpha}[(1-\frac{r_s}{4r})^{-2}(1+\frac{r_s}{4r})^2 + 2(1-\frac{r_s}{4r})^{-3}(1+\frac{r_s}{4r})^2]\frac{r_s}{4}\frac{\partial}{\partial x^\alpha}(\frac{1}{r}) \end{aligned} \tag{7.6}$$

and since

$$\begin{aligned} \frac{\partial}{\partial x^\alpha}(\frac{1}{r}) &= \frac{\partial}{\partial x^\alpha}[(x^2+y^2+z^2)^{-\frac{1}{2}}] \\ &= -\frac{1}{2}[(x^2+y^2+z^2)^{-\frac{3}{2}}]2x^\alpha \\ &= -(r^2)^{-\frac{3}{2}}x^\alpha \\ &= -r^{-3}x^\alpha \\ &= \frac{1}{r^3}x^\alpha \end{aligned} \tag{7.7}$$

The equation is reduced to

$$\frac{\partial g^{00}}{\partial x^\alpha} = \frac{1}{2r^3}[\frac{(1+\frac{r_s}{4r})}{(1-\frac{r_s}{4r})^2} + \frac{(1+\frac{r_s}{4r})^2}{(1-\frac{r_s}{4r})^3}]r_s x^\alpha \tag{7.8}$$

and can be further reduced by simplifying the term in the bracket

$$\begin{aligned}[\frac{(1+\frac{r_s}{4r})}{(1-\frac{r_s}{4r})^2}+\frac{(1+\frac{r_s}{4r})^2}{(1-\frac{r_s}{4r})^3}] &= \frac{(1+\frac{r_s}{4r})(1-\frac{r_s}{4r})}{(1-\frac{r_s}{4r})^3}+\frac{(1+\frac{r_s}{4r})^2}{(1-\frac{r_s}{4r})^3} \\ &= \frac{(1+\frac{r_s}{4r})(1-\frac{r_s}{4r})+(1+\frac{r_s}{4r})^2}{(1-\frac{r_s}{4r})^3} \\ &= (1+\frac{r_s}{4r})\frac{(1-\frac{r_s}{4r})+(1+\frac{r_s}{4r})}{(1-\frac{r_s}{4r})^3} \\ &= 2\frac{(1+\frac{r_s}{4r})}{(1-\frac{r_s}{4r})^3}\end{aligned} \tag{7.9}$$

$$\begin{aligned}\frac{\partial g^{11}}{\partial x^\alpha}=\frac{\partial g^{22}}{\partial x^\alpha}=\frac{\partial g^{33}}{\partial x^\alpha} &= \frac{\partial}{\partial x^\alpha}[-(1+\frac{r_s}{4r})^{-4}] \\ &= 4(1+\frac{r_s}{4r})^{-5}\frac{r_s}{4}\frac{\partial}{\partial x^\alpha}(\frac{1}{r}) \\ &= -\frac{1}{r^2}(1+\frac{r_s}{4r})^{-5}r_s x^\alpha\end{aligned} \tag{7.10}$$

The momentum can be found from the metric derivatives we have just solved for. By expanding the Einstein summation notation,

$$\frac{\partial p_\alpha}{\partial \zeta} = -\frac{1}{2}\frac{\partial g^{00}}{\partial x^\alpha}p_0p_0-\frac{1}{2}\frac{\partial g^{11}}{\partial x^\alpha}p_1p_1-\frac{1}{2}\frac{\partial g^{22}}{\partial x^\alpha}p_2p_2-\frac{1}{2}\frac{\partial g^{33}}{\partial x^\alpha}p_3p_3 \tag{7.11}$$

and recognizing that

$$\begin{aligned}p^2 &= p_1^2+p_2^2+p_3^2 \\ \frac{\partial g^{11}}{\partial x^\alpha} &= \frac{\partial g^{22}}{\partial x^\alpha}=\frac{\partial g^{33}}{\partial x^\alpha}\end{aligned} \tag{7.12}$$

where the superscript 2 on the momentums are powers in this instance. Since the spatial metric derivatives are equivalent, we arbitrarily choose them to be g^{11} so we may factor giving

$$= -\frac{1}{2}\frac{\partial g^{00}}{\partial x^\alpha}p_0^2-\frac{1}{2}\frac{\partial g^{11}}{\partial x^\alpha}p^2 \tag{7.13}$$

and since $p_0 \equiv -1$, we obtain the equations for momentum

$$-\frac{1}{2}[\frac{\partial g^{00}}{\partial x^\alpha}+\frac{\partial g^{11}}{\partial x^\alpha}p^2] \tag{7.14}$$